INFORMATICS JOURNALS

Research Article

Journal of Natural Remedies
DOI: 10.18311/jnr/2026/53880

eISSN: 2320-3358 | Vol 26(3), 2026 | pp. 699-712

# Formulation and *In Vitro* Evaluation of Diacerein Curcumin-loaded Hyaluronic Acid Nanogel

**Akanksha Chandra*** and **Rishabha Malviya**

Department of Pharmacy, School of Medical and Allied Sciences, Galgotias University, Greater Noida - 201310, Uttar Pradesh, India; chandraakshu55@gmail.com

## Abstract

**Background:** Diacerein (DCR), an anti-osteoarthritic agent, and curcumin, a natural anti-inflammatory compound, exhibit therapeutic potential; However, their clinical application is limited by poor bioavailability and stability. Hyaluronic Acid (HA)-based vesicular systems can enhance drug retention, hydration, and sustained release, making them suitable carriers for topical arthritis therapy. **Aim:** The present study aimed to develop and evaluate a novel topical gel formulation incorporating DCR-loaded HA vesicles and curcumin to achieve enhanced and sustained therapeutic efficacy in arthritis management. **Methods:** HA-based vesicles loaded with DCR were prepared using soy lecithin and evaluated for Particle Size (PS), Zeta Potential (ZP), Entrapment Efficiency (EE), and *in vitro* drug release. Based on optimisation studies, formulation F7 containing 0.4% (w/v) HA and 1 mg/mL DCR was selected and incorporated into a curcumin gel. The resulting gel was assessed for physicochemical properties, including pH, viscosity, drug content uniformity, spreadability, and *in vitro* drug release. **Results:** The optimised HA vesicle formulation (F7) showed a mean PS of 315nm, ZP of −12.3mV, EE of 91.3%, and sustained DCR release of 53% over 24 hours. The final DCR-loaded HA–curcumin gel exhibited a smooth and homogeneous texture with a pH of 6.4 ± 0.1, viscosity of 32,500 ± 500cps, and high drug content uniformity. *In vitro* release studies demonstrated controlled release of both drugs, with 65.4 ± 2.1% of curcumin and 48.7 ± 1.9% of DCR released over 24 hours. **Conclusion:** The developed DCR-loaded HA-curcumin gel demonstrated favourable physicochemical characteristics, high EE, and sustained, controlled drug release. The incorporation of HA enhanced drug retention, hydration, and stability, contributing to prolonged therapeutic effects. These findings suggest that the formulation has strong potential as a biocompatible topical treatment for arthritis, although further *in vivo* and clinical studies are required to confirm its efficacy and safety.

**Major Findings:** The optimised DCR-loaded hyaluronic acid vesicles (F7) showed high entrapment efficiency, favourable physicochemical properties, and sustained drug release. The final HA-Curcumin gel demonstrated suitable stability, uniformity, and controlled dual-drug release, indicating strong potential as a topical arthritis treatment.

**Keywords:** Arthritis, Curcumin, Diacerein, Hyaluronic Acid, Sustained Release, Topical Drug Delivery

**Abbreviations:** HA: Hyaluronic Acid; DCR: Diacerein; IL-1β: Interleukin-1 beta; EE: Entrapment Efficiency; TEM: Transmission Electron Microscopy; MWCO: Molecular Weight Cut-Off; PS: Particle Size; ZP: Zeta Potential; PDI: Polydispersity Index; ANOVA: Analysis of Variance.

(Article Chronicle: Article Received on: 02.12.2025; Revised on: 06.03.2026; Accepted on: 10.03.2026)

## 1. Introduction

Nanoparticulate drug delivery systems, particularly nanogels, offer significant advantages over conventional pharmaceutical formulations[1]. These benefits include enhanced drug encapsulation, prolonged circulation half-life, and precisely controlled or stimulus-triggered drug release mechanisms. Furthermore, the inherent design flexibility of nanogels allows for their precise functionalization to respond to specific physiological stimuli, such as variations in pH, temperature, or the presence of specific enzymes, thereby enabling targeted and site-specific drug delivery. Polymeric nanoparticles, which encompass nanogels, have demonstrated remarkable versatility as carriers for a diverse range of therapeutic and imaging

*Author for correspondence

agents. This versatility translates to improved drug distribution and augmented potency when compared to the administration of free therapeutic compounds[1]. Consequently, the capacity of nanogels to encapsulate a broad spectrum of active agents, including small molecules, biomacromolecules, and imaging probes, positions them as exceptionally promising vehicles for advanced drug delivery strategies.

HA has garnered substantial scientific interest in pharmaceutical applications due to its intrinsic biocompatibility, biodegradability, and non-immunogenicity, positioning it as an advantageous polymer for advanced drug delivery systems[2,3]. Its capacity for deep dermal penetration further establishes HA as a promising candidate for topical drug delivery formulations[4,5]. Moreover, HA's selective binding affinity for specific receptors on disease-relevant cells, such as cancer cells and activated macrophages, augments its utility in targeted drug delivery through facilitated receptor-mediated endocytosis[6]. The advent of nanotechnology has profoundly influenced drug delivery, facilitating the reduction of therapeutic dosages and mitigating adverse reactions, thereby enhancing overall treatment efficacy and patient adherence[7]. Nanoparticles, characterised by dimensions typically ranging from 10 to 1000nm, possess distinctive properties that render them highly suitable for pharmaceutical applications[8]. Among these, nanogels represent a sophisticated class of hydrogels with nanoscale dimensions, integrating the benefits of both hydrogels and nanoparticles. They are distinguished by high water absorptivity, excellent biocompatibility, flexibility, and a porous internal structure, which collectively make them ideal for encapsulating and delivering therapeutic agents[9].

DCR is classified as a symptomatic slow-acting drug primarily utilised in the therapeutic management of hip and knee osteoarthritis. Its mechanistic action involves the potent inhibition of interleukin-1 beta (IL-1β) production, a critical pro-inflammatory cytokine centrally involved in cartilage degradation and the inflammatory cascade[10]. By attenuating IL-1β activity, DCR effectively mitigates inflammation and contributes to chondroprotection.

The European Society for Clinical and Economic Aspects of Osteoporosis and Osteoarthritis positions DCR as a first-line pharmacological background treatment for osteoarthritis, particularly for patients where non-steroidal anti-inflammatory drugs or paracetamol are contraindicated[11]. Clinical trials have consistently demonstrated DCR's efficacy in reducing pain and improving joint function in osteoarthritis patients, with some studies suggesting a potential chondroprotective effect. However, it is important to note that DCR exhibits a slow onset of action, often requiring several weeks or months for its full therapeutic benefits to manifest, and its use is commonly associated with gastrointestinal side effects[11].

Curcumin, a natural polyphenol derived from turmeric, demonstrates a wide spectrum of therapeutic properties, including potent anti-inflammatory, antioxidant, and anti-cancer effects. Its anti-inflammatory action is primarily attributed to its capacity to suppress pro-inflammatory cytokines, chemokines, and enzymes[12]. Furthermore, curcumin inhibits inflammatory pathways by modulating inflammatory mediators.

Despite these promising attributes, curcumin's therapeutic utility is significantly constrained by its inherent limitations, such as poor aqueous solubility, rapid metabolism, and low bioavailability, which collectively hinder its clinical application. To surmount these challenges, the implementation of nanotechnology in curcumin delivery aims not only to address issues of solubility, metabolic stability, and drug stability but also to facilitate targeted delivery to specific tissues, thereby minimising unintended effects on healthy cells[13]. The combination of curcumin and DCR in a single formulation offers a synergistic approach to treating inflammatory conditions, leveraging the anti-inflammatory and antioxidant properties of both drugs, which may allow for reduced dosages of each drug, potentially minimising side effects while maximising therapeutic benefits[14]. Additionally, nanogel formulations are recognised for their potential to improve the stability, solubility, and bioavailability of both curcumin and DCR.

## 2. Materials and Methods

### 2.1 Materials

DCR was provided as a gift sample from Rakshit Drugs Pvt Ltd, Hyderabad, India. Tween 80, HA (low molecular weight), was procured from Himedia (India).

Poloxamer 407 and ethanol were purchased from Merck (India). Curcumin was procured from Sigma-Aldrich (Mumbai, India). All the other chemicals used were of analytical grade.

## 2.2 Methods

### 2.2.1 Design of Experiments

A comprehensive experimental design, specifically the Box–Behnken design, was strategically employed to optimise the formulation of DCR-loaded nanovesicles. This robust design facilitated the systematic evaluation of three critical independent factors: HA concentration, drug concentration, and sonication time. These factors were assessed for their impact on key dependent variables (responses), namely mean Vesicle Size (Y1), Entrapment Efficiency (Y2), and Zeta Potential (Y3). The specific constraints and optimisation goals established for these dependent variables are meticulously detailed in Table 1 of the study. Subsequently, a total of twelve distinct formulations, representing various combinations derived from the Box Behnken Design (BBD), were prepared and analysed in a fully randomised order, as delineated in Table 2.

**Table 1.** Independent and dependent variables used in the Box-Behnken design for the formulation of DCR-loaded nanovesicles

| Independent Variables | Levels | | |
|---|---|---|---|
| | -1 | 0 | +1 |
| $X_1$: Concentration of HA (%) | 0.2 | 0.5 | 0.8 |
| $X_2$: Drug Concentration (mg/ml) | 0.5 | 1.25 | 2.0 |
| $X_3$: Sonication Time (min) | 2.5 | 3.75 | 5.0 |
| **Dependent Variables** | **Constraints** | | |
| | **Low** | **High** | **Goal** |
| R1: Mean Vesicle Size (nm) | 308 | 364 | Minimise |
| R2: Entrapment Efficiency (%) | 78.6 | 94.2 | Maximise |
| R3: ZP | -11.5 | -14.6 | Minimise |

### 2.2.2 Preparation of DCR-loaded HA Nanovesicles

Diacerein-loaded Nanovesicles (DCN) were prepared using the thin-film hydration technique. This involved the precise integration of soya lecithin as the foundational lipid matrix and Tween 80 as a crucial edge activator. The lipid components were used at an optimised molar ratio of 85:15, comprising 200mg of soya lecithin, 28.2mg of Tween 80, and the requisite quantity of DCR[15].

These constituents were completely dissolved in 10mL of a chloroform: methanol mixture, ensuring homogeneous solubilisation of both lipids and the therapeutic agent[16,17]. The resulting organic phase then underwent rotary evaporation under vacuum at 50°C for 15 minutes at 150rpm. This controlled evaporation facilitated the efficient removal of organic solvents and promoted the deposition of a thin, uniform lipid film along the inner surface of the flask[18,19].

Subsequently, the desiccated lipid film was hydrated with 10mL of phosphate-buffered saline (PBS, pH

**Table 2.** Composition of different DCR-loaded HA vesicular formulations

| Std | Run | X1: Hydration Media (%) | X2:Drug Concentration (mg/ml) | X3: Sonication time (min) | R1: PS (nm) | R2: EE% | R3: ZP (mV) |
|---|---|---|---|---|---|---|---|
| 9 | 1 | 0.5 | 0.5 | 2.5 | 352 | 81.7 | -14.6 |
| 10 | 2 | 0.5 | 2 | 2.5 | 358 | 92.4 | -13.1 |
| 3 | 3 | 0.2 | 2 | 3.75 | 334 | 94.2 | -11.6 |
| 12 | 4 | 0.5 | 2 | 5 | 318 | 78.6 | -12.7 |
| 6 | 5 | 0.8 | 1.25 | 2.5 | 358 | 92.5 | -14.1 |
| 11 | 6 | 0.5 | 0.5 | 5 | 340 | 78.6 | -11.9 |
| 4 | 7 | 0.8 | 2 | 3.75 | 356 | 91.3 | -13.4 |
| 2 | 8 | 0.8 | 0.5 | 3.75 | 364 | 83.2 | -13.1 |
| 5 | 9 | 0.2 | 1.25 | 2.5 | 352 | 84.5 | -12.1 |
| 8 | 10 | 0.8 | 1.25 | 5 | 325 | 81.7 | -12.3 |
| 7 | 11 | 0.2 | 1.25 | 5 | 308 | 78.6 | -11.5 |
| 1 | 12 | 0.2 | 0.5 | 3.75 | 316 | 83.4 | -14.2 |

7.4), containing predetermined concentrations of HA, which served as the hydrating medium. The hydration process was further enhanced by sonicating the flask for 5 minutes, culminating in the formation of a milky dispersion of DCN-loaded hyaluosomes[20,21]. This resultant dispersion was then subjected to comprehensive characterisation as per the experimental design.

### 2.2.3 Characterisation of the Prepared DCN-loaded HA Vesicles

#### 2.2.3.1 Determination of Entrapment Efficiency (EE%)

The EE% of DCR within the prepared HA vesicles was rigorously quantified using an indirect method. This approach was predicated on the precise measurement of the free, unencapsulated drug present in the dispersion medium. Specifically, a 1 mL aliquot of the freshly formulated DCR-loaded HA vesicle dispersion was subjected to ultracentrifugation at 22,000rpm for 1 hour at a controlled temperature of 4°C, utilising a refrigerated centrifuge. This critical step facilitated the efficient sedimentation of the HA vesicles, thereby enabling the effective separation of the free drug, which remained in the supernatant. The isolated supernatant was subsequently carefully withdrawn, appropriately diluted with phosphate-buffered saline, and quantitatively analysed spectrophotometrically using an Ultraviolet (UV)–Vis spectrophotometer at a maximum absorbance wavelength of 258 nm[22].

#### 2.2.3.2 Determination of Particle Size (PS), Zeta Potential (ZP), and Polydispersity Index (PDI)

The PS, ZP, and PDI of the DCR-loaded hyaluosomes were meticulously determined using dynamic light scattering via a Zetasizer Nano ZS[23]. Prior to analysis, each formulation was appropriately diluted with double-distilled water to achieve optimal scattering intensity and mitigate multiple scattering effects[24]. The diluted samples were subsequently introduced into disposable cuvettes for PS and PDI measurements, and into folded capillary cells for ZP analysis[25].

PS and PDI were calculated based on photon correlation spectroscopy, reflecting the hydrodynamic diameter and size distribution uniformity, respectively[26,27]. ZP, a crucial indicator of surface charge and colloidal stability, was determined by measuring the electrophoretic mobility of the particles under an applied electric field[28–33]. The absolute mean ZP values are often used as a rule of thumb to assess colloidal stability, with higher magnitudes suggesting greater stability due to increased repulsive interactions between particles[30]. Each sample was analysed in triplicate, and the results are expressed as the mean ± standard deviation.

#### 2.2.3.3. In Vitro Drug Release Evaluation of Optimised DCR-loaded HA Vesicles

The *in vitro* release profile of DCR from the optimised formulation was assessed using the dialysis bag diffusion technique[34] facilitated by a thermostatically controlled magnetic stirrer. Before experimentation, a cellulose dialysis membrane was pre-soaked in phosphate-buffered saline at pH 7.4 overnight to ensure optimal hydration and permeability. Subsequently, 1mL aliquots of the optimised DCR-loaded hyaluosome formulation, each containing 2 mg of DCR, were carefully introduced into the pre-soaked dialysis membranes. These membranes were then securely sealed and immersed in 20mL of PBS within 100mL conical flasks, maintained at 37 ± 0.5°C under continuous agitation by a magnetic stirrer to simulate physiological conditions.

At predetermined intervals, 1mL aliquots of the external release medium were precisely withdrawn and immediately replenished with an equal volume of fresh PBS, thereby maintaining sink conditions throughout the study. The quantitative determination of released DCR was performed spectrophotometrically at a maximum absorbance wavelength of 258nm. All experimental assays were conducted in triplicate, and the reported results are expressed as the mean ± standard deviation.

#### 2.2.3.4 Transmission Electron Microscopy (TEM) Analysis

The morphological characteristics of the optimised DCR-loaded HA vesicles were rigorously examined using TEM[35]. This involved meticulously placing a small aliquot of the undiluted vesicular dispersion onto a carbon-coated copper grid and allowing it to adsorb for 1–2 minutes. Excess liquid was subsequently removed via blotting with filter paper. To enhance contrast, the sample was then negatively stained with

a 1% (w/v) phosphotungstic acid solution, followed by air-drying at ambient temperature[36–38]. The prepared grids were examined under a Joel JEM 1230 TEM, operated at an accelerating voltage of 80 kV[39–42].

#### 2.2.4 Preparation of DCR-loaded HA-Curcumin Gel

The DCR-loaded HA–curcumin gel was meticulously formulated using Poloxamer 407, a well-established thermosensitive gelling agent, at a concentration of 18% (w/v). Initially, Poloxamer 407 was gradually dispersed in cold distilled water (4°C) under gentle stirring to prevent agglomeration. This dispersion was then stored overnight at 4±1 °C to ensure complete dissolution and optimal gel formation. Curcumin, at a concentration of 0.5% (w/v), was pre-dissolved in a minimal volume of ethanol to enhance its solubility and subsequently incorporated into the Poloxamer gel base under constant agitation to achieve uniform distribution.

Following this, the optimised DCR-loaded HA vesicles were carefully integrated into the Poloxamer-curcumin gel, while strictly maintaining the temperature below 10°C to preserve their vesicular integrity. The final DCR concentration in the resultant gel was precisely adjusted to 1% (w/w). Homogeneity was ensured by gently stirring the mixture for 10–15 minutes, after which the pH was adjusted to a skin-compatible range of 5.5–6.5 using triethanolamine[43,44]. The prepared gel was then stored in amber-colored, airtight containers at 4±1°C to maintain its stability and integrity.

#### 2.2.5 Evaluation of the Prepared DCR-loaded HA-Curcumin Gel

##### 2.2.5.1 Physical Appearance and Homogeneity

The prepared gel was visually inspected for colour, clarity, and the presence of any lumps, aggregates, or phase separation. Homogeneity was further assessed by applying a small quantity of gel between the fingers to check for smoothness and uniform texture[45].

##### 2.2.5.2 pH Measurement

The pH of the gel formulation was measured using a calibrated digital pH meter at room temperature. A small amount of gel was dispersed in distilled water (1:10 w/v), and the electrode was immersed in the solution. The measurement was recorded in triplicate, and the average value was reported[46].

##### 2.2.5.3 Viscosity and Rheological Behaviour

Viscosity was determined using a Brookfield viscometer equipped with a spindle #64. The gel sample was subjected to shear rates at 25±1°C to assess flow behaviour and viscosity. The rheological profile was used to determine whether the gel exhibited pseudoplastic, Newtonian, or thixotropic behavior[47].

##### 2.2.5.4 In Vitro Drug Release Study: DCR and Curcumin from the Gel

The *in vitro* release of DCR and curcumin from the gel was evaluated using the dialysis bag diffusion method. A dialysis membrane (MWCO~12,000 Da) was presoaked overnight in PBS (pH 7.4). Approximately 1g of gel containing known amounts of drugs was placed inside the dialysis bag, which was then immersed in 100 mL of PBS (pH 7.4) maintained at 37±0.5°C with continuous stirring at 50rpm. At predetermined time intervals, 2mL aliquots of the release medium were withdrawn and replaced with fresh buffer to maintain sink conditions. The amount of drug released was quantified using UV–Vis spectrophotometry at the wavelengths 258 for DCR and 424nm for curcumin[48]. All tests were conducted in triplicate, and cumulative release was calculated.

## 3. Results and Discussion

### 3.1 Optimisation of DCR-loaded HA Vesicles: Entrapment Efficiency (EE%), Particle Size (PS), Zeta Potential (ZP), and Polydispersity Index (PDI)

DCR-loaded HA vesicles were successfully formulated using the thin film hydration technique, and their composition was optimised through Design-Expert® version 13.0 software (Stat-Ease Inc., Minneapolis, MN, USA). A factorial design was employed to statistically assess the influence of key formulation variables on critical quality attributes like EE%, PS, ZP, and PDI.

As presented in Table 2, all prepared formulations exhibited notable EE% values ranging from 78.6% to 94.2%, confirming efficient drug loading. The PS of the HA vesicles were in the nanometric range (300-400nm), suitable for topical delivery and skin

permeation. The formulations demonstrated acceptable size distribution, with PDI values between 0.2 and 0.4, indicating moderately uniform particle populations. Additionally, all vesicles exhibited a negative surface charge, with ZP values ranging from -11.5 to -14.6mV, suggestive of good colloidal stability due to electrostatic repulsion.

The results indicate that mean vesicle size is adequately described by a linear relationship within the studied factor range. The linear model showed a significant sequential p-value (p = 0.0062), indicating that the inclusion of linear terms resulted in a meaningful improvement over a null model. In addition, the lack of fit test for the linear model was not significant (p = 0.6834), suggesting that the model adequately describes the experimental data and that no systematic variation remains unexplained. The adjusted $R^2$ value of 0.4818 indicates that approximately 48% of the variability in mean vesicle size can be explained by the linear effects of the studied factors (Table 3). Furthermore, the predicted $R^2$ was acceptable, demonstrating that the model has reasonable predictive performance for new observations within the design space.

The linear model demonstrated a statistically significant sequential p-value (p = 0.0250), indicating that the inclusion of linear terms significantly improved the model compared to a null model. The lack of fit test was not significant (p = 0.5463), suggesting that the linear model adequately represents the experimental data and that no substantial unexplained systematic variation remains. The adjusted $R^2$ value of 0.2576 indicates that approximately 26% of the variability in the response is explained by the linear effects of the factors studied (Table 3).

The 3D surface plot illustrates the combined effect of $X_1$: Concentration of HA (%) and $X_2$: Drug concentration (mg/mL) on EE(%), while the third factor (C) is held constant at 3.75. The response surface demonstrates a gradual change in EE across the experimental domain.

An increase in both HA concentration and drug concentration results in a noticeable improvement in EE. Lower levels of HA and drug concentration correspond to reduced EE, whereas higher levels of these factors lead to higher efficiency values. This trend suggests that HA concentration plays an important role in enhancing drug encapsulation, likely due to increased matrix formation and improved drug–polymer interactions. Similarly, increasing drug concentration provides greater availability of the drug for incorporation into the vesicles.

The linear model showed a non-significant sequential p-value (p = 0.0911), indicating that the linear terms alone did not sufficiently explain the variability in the response. Although the lack of fit test was not significant (p = 0.3604), suggesting an acceptable fit, the adjusted $R^2$ value was slightly negative (−0.0466), indicating that the model performed worse than a

**Table 3.** Fit summary of the developed statistical models showing regression and ANOVA parameters for response 1 (mean vesicle size), response 2 (EE), and response 3 (ZP)

| Response 1: Mean Vesicle Size | | | | | |
|---|---|---|---|---|---|
| **Source** | **Sequential p-Value** | **Lack of Fit p-Value** | **Adjusted $R^2$** | **Predicted $R^2$** | |
| **Linear** | **0.0062** | | **0.6834** | **0.4818** | **Suggested** |
| 2FI | 0.4013 | | 0.7048 | 0.2271 | |
| Quadratic | 0.7088 | | 0.6089 | -0.7068 | **Aliased** |
| **Response 2: Entrapment Efficiency** | | | | | |
| **Linear** | **0.0250** | | **0.5463** | **0.2576** | **Suggested** |
| 2FI | 0.6070 | | 0.4818 | -0.3567 | |
| Quadratic | 0.2248 | | 0.6807 | -0.3933 | **Aliased** |
| **Response 3: Zeta Potential** | | | | | |
| **Linear** | 0.0911 | | 0.3604 | -0.0466 | |
| **2FI** | **0.1066** | | **0.6684** | **0.1319** | **Suggested** |
| Quadratic | 0.3685 | | 0.7159 | -0.2395 | **Aliased** |

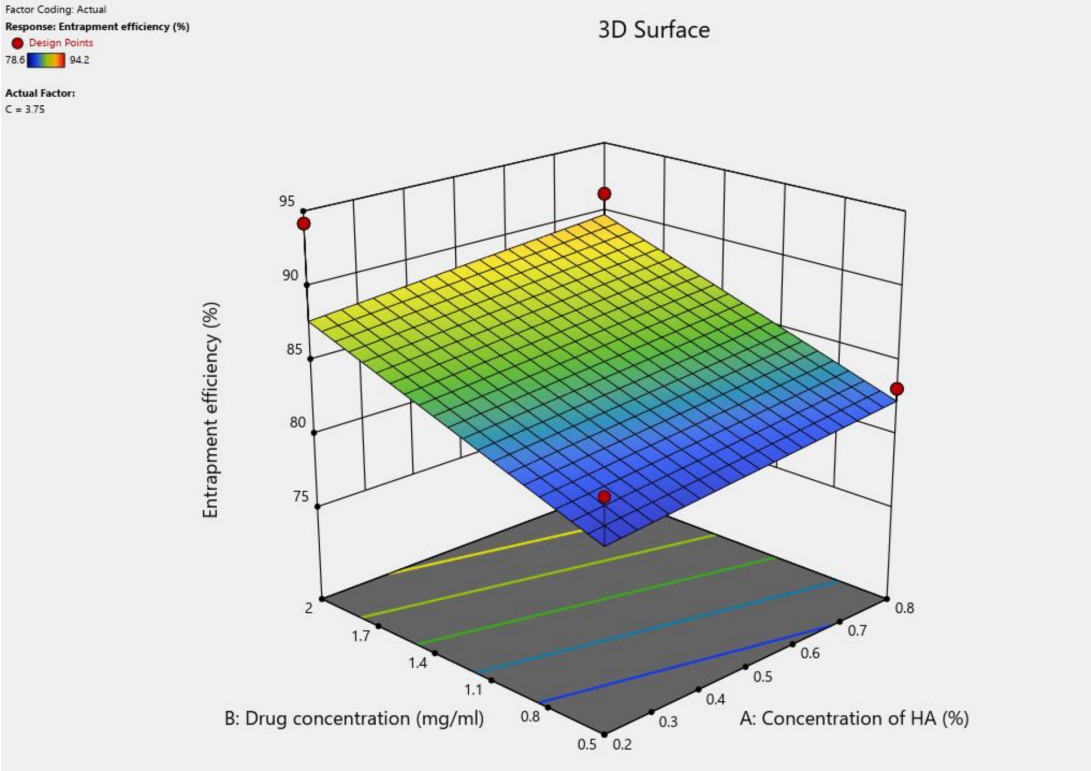



**Figure 1.** 3D response surface plot showing the combined effect of HA concentration ($X_1$, %) and drug concentration ($X_2$, mg/mL) on EE (%).

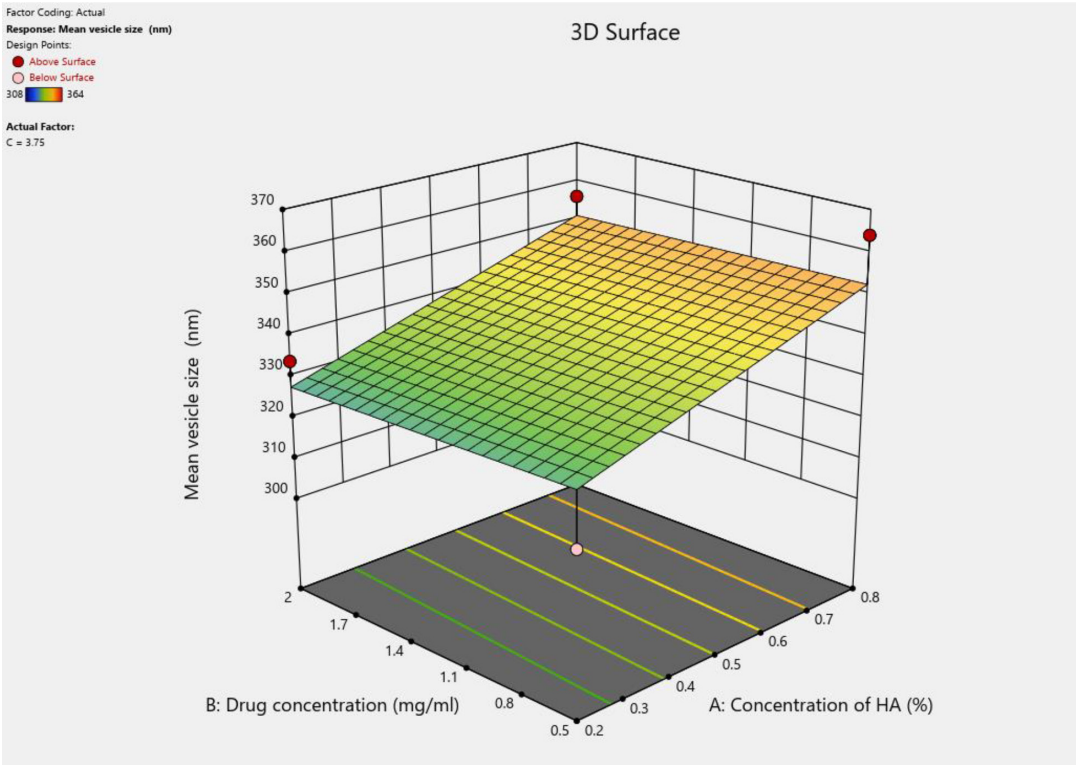



**Figure 2.** 3D response surface plot showing the combined effect of HA concentration ($X_1$, %) and drug concentration ($X_2$, mg/mL) on mean vesicle size.

simple mean-based model (Table 3). This reflects the limited explanatory power of the linear effects within the studied factor range.

Analysis of Variance (ANOVA) was used to evaluate the statistical significance of formulation variables. Results indicated that both drug concentration ($p < 0.0001$) and HA concentration ($p = 0.0067$) had significant effects on EE%. As shown in Figure 1, increasing the concentration of DCR led to enhanced drug entrapment, likely due to the hydrophobic nature of DCR, which favours its incorporation within the lipid bilayer of vesicles.

Moreover, increasing the concentration of HA also resulted in a significant enhancement in EE%. This effect may be ascribed to the steric stabilisation provided by the long polysaccharide chains of HA, which extend outward from the vesicle surface, effectively reducing drug leakage by creating a physical barrier. These findings align with prior work by Hanieh *et al.*, who demonstrated that the incorporation of HA into liposomal formulations produced more stable vesicles with reduced drug leakage and lower aggregation tendencies, supporting the formation of robust HA vesicles[49].

None of the evaluated formulation variables exerted a statistically significant effect on the PS or the PDI of the prepared DCR-loaded HA vesicles, as indicated by p-values > 0.05. This suggests that within the tested ranges, the selected factors did not markedly influence vesicle size or distribution uniformity (Figure 2).

Regarding the ZP, all formulations exhibited a negative surface charge, which can be attributed to the inherent anionic nature of soya lecithin and HA, both of which contribute negatively charged functional groups to the vesicle surface. Among the tested variables, only HA concentration demonstrated a statistically

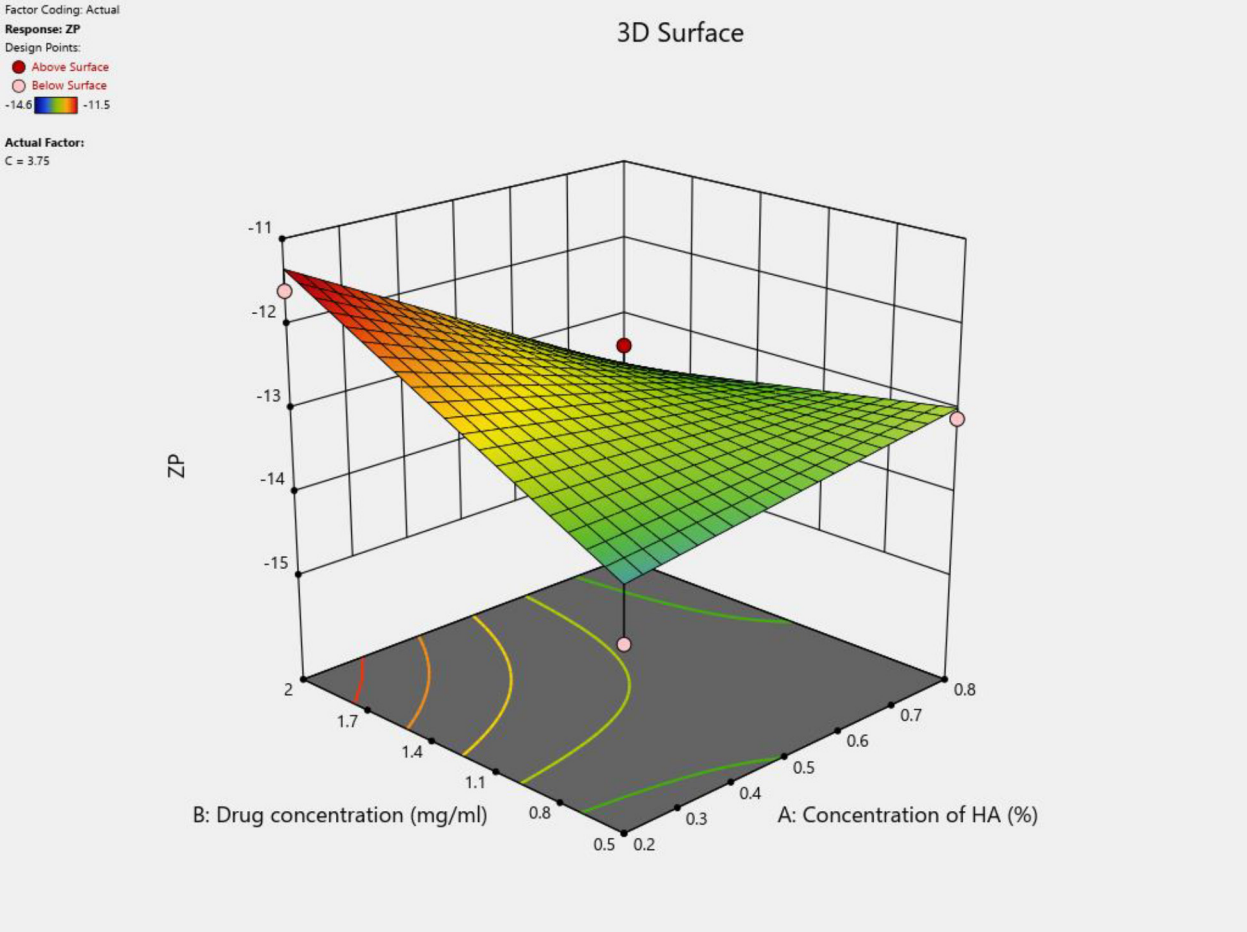



**Figure 3.** 3D response surface plot showing the combined effect of HA concentration ($X_1$, %) and drug concentration ($X_2$, mg/mL) on zeta potential.

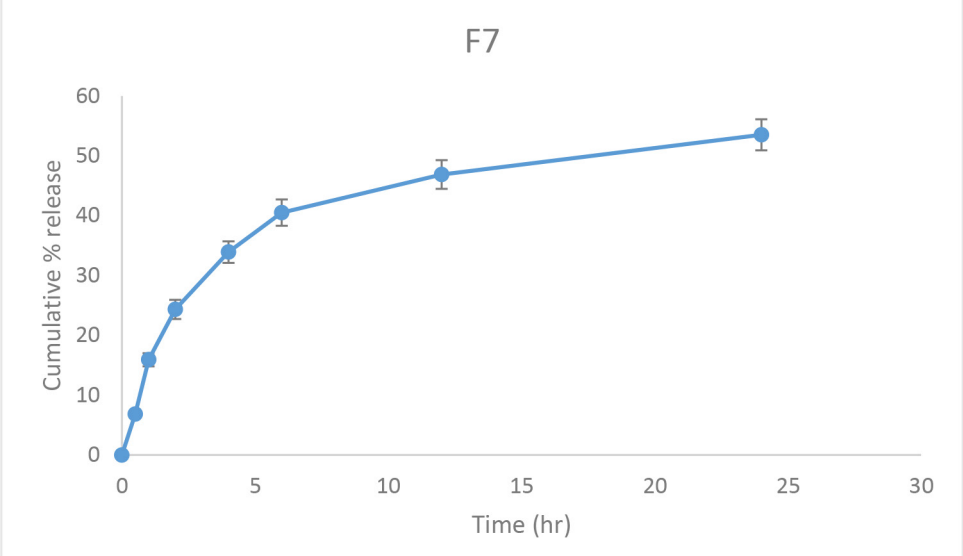



**Figure 4.** *In vitro* drug release profile of diacerein from the optimised DCR-loaded HA vesicles (F7).

significant influence on ZP ($p = 0.0128$), as confirmed by ANOVA. As shown in Figure 3, increasing the HA concentration resulted in a significant increase in the magnitude of the negative ZP. This observation can be attributed to the increased density of negatively charged carboxyl and hydroxyl groups present on the HA polymer chains, which become more prominent on the vesicle surface at higher HA levels, thereby enhancing the net negative surface charge[50].

## 3.2 *In Vitro* Drug Release from the Optimised HA Vesicles

The *in vitro* release profile of DCR from the optimised DCR-loaded HA vesicles (F7) was determined. The percentage of drug released at predetermined time intervals is illustrated in Figure 1. The data clearly demonstrate that the optimised formulation significantly sustained the release of DCR over time. Specifically, the optimised HA vesicle formulation (F7) released around 53.51% of the total drug content over 24 hours (Figure 4). This pronounced delay in release kinetics is indicative of the controlled release potential of the HA vesicular system.

The sustained release behaviour of the HA vesicles can be attributed to the presence of soya lecithin, which forms a lipid bilayer that serves as a barrier to diffusion, thereby slowing the ingress of the dissolution medium and subsequent drug release. Furthermore, the incorporation of HA adds a structural and functional dimension. Due to its high molecular weight and extended sugar chains, HA may remain partially embedded within the bilayer while also projecting outward from the vesicle surface. This steric hindrance effect likely contributes to enhanced vesicle stability and further retardation of drug diffusion, resulting in prolonged release kinetics[51].

## 3.3 Transmission Electron Microscopy (TEM)

TEM analysis was performed to investigate the morphological characteristics of the optimised DCR-loaded HA vesicles. As shown in Figure 5, the micrographs revealed well-defined, spherical vesicles with smooth surfaces, distinct boundaries, and no evidence of aggregation, indicating good colloidal stability. The PS observed in the TEM images were in close agreement with those obtained via dynamic light scattering (Zetasizer), confirming the nanometric scale and uniformity of the vesicular systems. The morphological integrity and well-organised structure of the HA-containing vesicles further support their potential for sustained and targeted topical delivery.

## 3.4 Evaluation of the Prepared DCR-loaded HA-Curcumin Gel

The formulated DCR-loaded HA-Curcumin gel was evaluated for various physicochemical parameters to

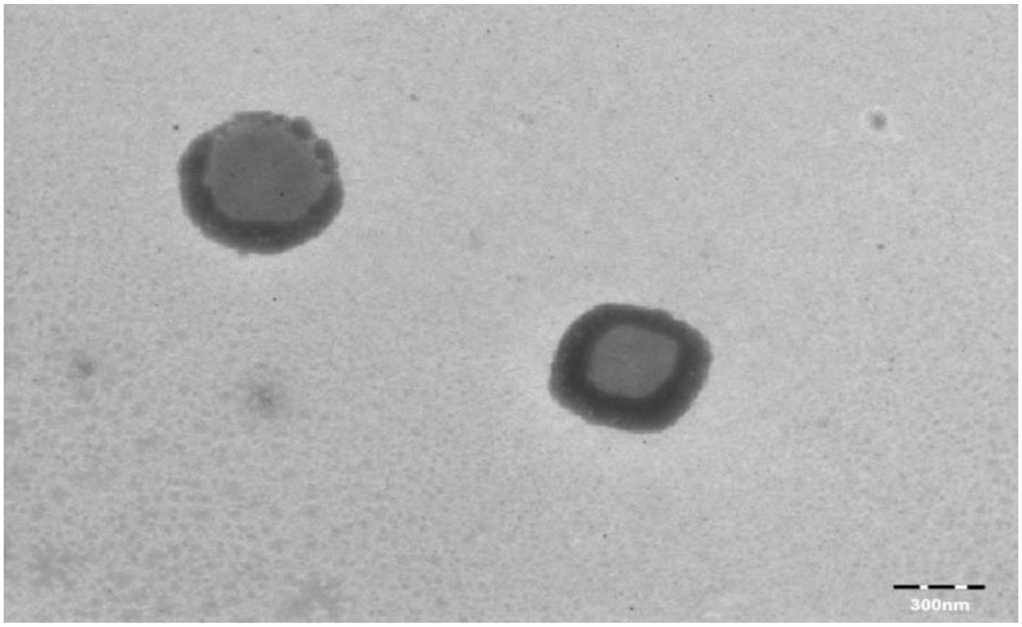



**Figure 5.** TEM photograph of DCR-loaded HA vesicles.

determine its suitability for topical application. The following results were obtained:

### 3.4.1 Physical Appearance

The prepared gel was observed to be smooth, homogenous, and free from lumps or grittiness. It exhibited a light yellow to amber colouration, attributed to the curcumin content, and had no signs of phase separation or microbial growth during initial observation.

### 3.4.2 pH Measurement

The pH of a topical formulation is a critical parameter that directly affects its compatibility with the skin and its overall stability. In this study, the prepared DCR-loaded HA-Curcumin gel exhibited a pH of 6.4 ± 0.1, which falls within the physiologically acceptable range for topical applications (typically between pH 4.5 and 7.0). Human skin has a slightly acidic surface pH, generally around 5.5. However, formulations with a pH up to 6.5 are often considered safe and non-irritating, especially when they contain buffering or soothing agents like HA, which can help maintain skin hydration and barrier function. The observed pH value ensures minimal risk of irritation or disruption to the skin's natural acid mantle, which is essential for maintaining microbial balance and protective functions. Additionally, the pH value supports the chemical stability of both curcumin and DCR in the gel matrix. Curcumin is known to degrade in highly alkaline environments; thus, maintaining a slightly acidic to neutral pH helps to preserve its bioactivity. The consistency of the pH reading (±0.1) also suggests good formulation reproducibility and stability.

### 3.4.3 Viscosity

Viscosity and rheological behaviour play a pivotal role in the performance and user acceptability of topical gel formulations. The viscosity of the DCR-loaded HA-Curcumin gel was determined to be 32,500 ± 500 cps at 25°C, using a Brookfield viscometer. This value indicates that the gel possesses a semi-solid consistency that is ideal for topical application. A formulation with this viscosity provides a balanced profile between spreadability and retention. It is thick enough to remain localised on the application site without immediate runoff, thus ensuring prolonged contact and better drug absorption, yet not too viscous to hinder smooth application or patient compliance. This is especially important for active compounds like curcumin and DCR, which benefit from sustained release and local retention.

The presence of HA likely contributed to the gel's viscosity by forming a structured network within the gel matrix. HA is a known rheology modifier and also enhances skin hydration, which may improve the therapeutic effect and skin feel of the gel. The measured viscosity suggests that the gel likely exhibits pseudoplastic behaviour, a desirable trait for topical formulations. Such behaviour ensures that the gel spreads easily under shear (e.g., during application) but maintains its structure afterwards, enhancing both functionality and user comfort.

### 3.4.4 *In Vitro* Drug Release Profile of the DCR-loaded HA-Curcumin Gel

*In vitro* drug release profile of the DCR-loaded HA-Curcumin gel was evaluated to assess the formulation's ability to provide sustained drug delivery over an extended period. Over 24 hours, the gel demonstrated a controlled and sustained release pattern, with 65.4 ± 2.1% of curcumin and 48.7 ± 1.9% of DCR released (Table 4 and Figure 6).

**Table 4.** *In vitro* drug release profile of the DCR-loaded HA-Curcumin gel

| Time (hrs) | % Curcumin Released (Mean ± SD) | % DCR Released (Mean ± SD) |
|---|---|---|
| 0 | 0 | 0 |
| 1 | 12.3 ± 0.8 | 12.5 ± 0.7 |
| 2 | 19.6 ± 1.1 | 19.4 ± 0.9 |
| 4 | 32.5 ± 1.4 | 30.2 ± 1.2 |
| 6 | 41.8 ± 1.7 | 38.1 ± 1.5 |
| 12 | 59.3 ± 2.0 | 43.8 ± 1.7 |
| 24 | 65.4 ± 2.1 | 48.7 ± 1.9 |

The release pattern suggests a biphasic profile, with an initial moderate release in the first few hours, likely due to surface-associated drug diffusing into the medium, followed by a slower, sustained release attributed to drug diffusion through the gel matrix. This behaviour is advantageous for topical therapies requiring prolonged action, as it ensures continuous drug availability at the site of application without the need for frequent reapplication.

The incorporation of HA likely contributed to the sustained release characteristics. HA's high molecular weight and hydrophilic nature help form a hydrated gel network that can act as a diffusion barrier, modulating the release of both curcumin and DCR. Additionally, the gel's viscosity, previously measured at 32,500 ± 500 cps, supports the idea of a dense matrix capable of retarding drug diffusion. The controlled release of curcumin is particularly beneficial, as it improves its therapeutic efficacy and minimises degradation, given curcumin's known instability under physiological conditions. Similarly, sustained release of DCR enhances its therapeutic window while potentially reducing systemic exposure and side effects.

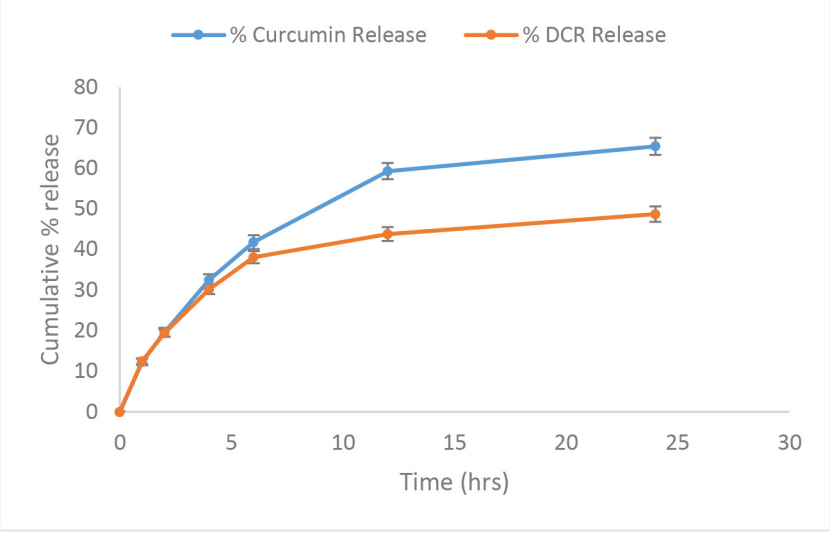



**Figure 6.** *In vitro* drug release profile of the DCR-loaded HA-Curcumin gel.

## 4. Conclusion

In this study, DCR-loaded HA vesicles were successfully formulated and characterised. The optimised HA vesicle formulation demonstrated physicochemical properties, including PS, ZP, and EE, conducive to effective drug delivery. These vesicles also exhibited a sustained release profile for DCR over a 24-hour period.

Subsequently, these optimised DCR-loaded HA vesicles were incorporated into a thermosensitive Poloxamer 407-based curcumin gel. The resulting gel formulation was evaluated for its physical appearance, homogeneity, pH, and viscosity, all of which indicated its suitability for topical application. *In vitro* drug release studies of the combined gel confirmed a controlled and sustained delivery of both DCR and Curcumin over 24 hours. This sustained release mechanism is likely facilitated by the structured gel matrix, particularly the HA component, which can enhance drug retention and skin hydration at the application site.

Overall, the developed DCR-loaded HA-Curcumin gel presents a stable, biocompatible, and effective system with significant potential for improving the topical management of arthritis or related inflammatory conditions. The synergistic combination of DCR and curcumin, delivered through this advanced nanogel platform, holds promise for enhanced therapeutic efficacy. Further *in vivo* and clinical studies are essential to fully validate its therapeutic benefits and safety profile.

## 5. Acknowledgement

The authors extend their appreciation to the Department of Pharmacy, School of Medical and Allied Sciences, Galgotias University, Greater Noida, Uttar Pradesh, India, for providing all facilities to conduct the research work.

## 6. References

1. Jha A, Rama A, Ladani B, Verma N, Kannan S, Naha A. Temperature and pH-responsive nanogels as intelligent drug delivery systems: A comprehensive review. J Appl Pharm Sci. 2021. https://doi.org/10.7324/JAPS.2021.1101201
2. Kim K, Choi H, Choi ES, Park M-H, Ryu J-H. Hyaluronic acid-coated nanomedicine for targeted cancer therapy. Pharmaceutics. 2019; 11(7):301. https://doi.org/10.3390/pharmaceutics11070301 PMid:31262049 PMCid:PMC6680416.
3. Huang J, Li R, Cai J, Wang Y, Chen J, Zheng H. Effect of potential-determining ions on rheological properties of calcite paste. Materials (Basel). 2025; 18(9):2020. https://doi.org/10.3390/ma18092020 PMid:40363521 PMCid:PMC12072846.
4. Tripodo G, Trapani A, Torre ML, Giammona G, Trapani G, Mandracchia D. Hyaluronic acid and its derivatives in drug delivery and imaging: Recent advances and challenges. Eur J Pharm Biopharm. 2015; 97(PtB):400-416. https://doi.org/10.1016/j.ejpb.2015.03.032 PMid:26614559
5. Witting M, Boreham A, Brodwolf R, Vávrová K, Alexiev U, Friess W, *et al*. Interactions of hyaluronic Acid with the skin and implications for the dermal delivery of biomacromolecules. Mol Pharm. 2015; 12(5):1391-1401. https://doi.org/10.1021/mp500676e PMid:25871518.
6. Saravanakumar G, Deepagan VG, Jayakumar R, Park JH. Hyaluronic acid-based conjugates for tumour-targeted drug delivery and imaging. J Biomed Nanotechnol. 2014; 10(1):17-31. https://doi.org/10.1166/jbn.2014.1761 PMid:24724496.
7. Kadry MO, Abdel-Megeed RM. CRISPR-Cas9 genome and long non-coding RNAs as a novel diagnostic index for prostate cancer therapy via liposomal-coated compounds. PLoS One. 2024; 19(5):e0302264. https://doi.org/10.1371/journal.pone.0302264 PMid:38723038 PMCid:PMC11081254.
8. Rizvi SAA, Saleh AM. Applications of nanoparticle systems in drug delivery technology. Saudi Pharm J. 2018;26(1):64-70. https://doi.org/10.1016/j.jsps.2017.10.012 PMid:29379334 PMCid:PMC5783816.
9. Attama AA, Nnamani PO, Onokala OB, Ugwu AA, Onugwu AL. Nanogels as target drug delivery systems in cancer therapy: A review of the last decade. Front Pharmacol. 2022; 13:874510. https://doi.org/10.3389/fphar.2022.874510 PMid:36160424 PMCid:PMC9493206.
10. Kaur D, Kaur J, Kamal SS. Diacerein, its beneficial impact on chondrocytes and notable new clinical applications. Braz J Pharm Sci. 2018; 54(4). https://doi.org/10.1590/s2175-97902018000417534
11. Pavelka K, Bruyère O, Cooper C, Kanis JA, Leeb BF, Maheu E, *et al*. Diacerein: Benefits, risks and place in the management of osteoarthritis. An opinion-based report from the ESCEO. Drugs Aging. 2016; 33(2):75-85. https://doi.org/10.1007/s40266-016-0347-4 PMid:26849131 PMCid: PMC4756045.
12. Khatamsaz S, Hashemi M. Curcumin and curcumin-loaded nanogel induce apoptosis activity in K562 chronic myelogenous leukemia cells. Galen. 2018; 7:e921. https://doi.org/10.31661/gmj.v7i0.921

13. Navya PN, Kaphle A, Srinivas SP, Bhargava SK, Rotello VM, Daima HK. Current trends and challenges in cancer management and therapy using designer nanomaterials. Nano Converg. 2019; 6(1):23. https://doi.org/10.1186/s40580-019-0193-2 PMid:31304563 PMCid:PMC6626766.
14. Berretta M, Dal Lago L, Tinazzi M, Ronchi A, La Rocca G, Montella L, *et al*. Evaluation of concomitant use of anticancer drugs and herbal products: From interactions to synergic activity. Cancers (Basel). 2022; 14(21):5203. https://doi.org/10.3390/cancers14215203 PMid:36358622 PMCid:PMC9657145.
15. Saporito F, Sandri G, Bonferoni MC, Rossi S, Boselli C, Icaro Cornaglia A, *et al*. Essential oil-loaded lipid nanoparticles for wound healing. Int J Nanomedicine. 2018; 13:175-186. https://doi.org/10.2147/IJN.S152529 PMid:29343956 PMCid:PMC5747963.
16. Selyanchyn O, Bayer T, Klotz D, Selyanchyn R, Sasaki K, Lyth SM. Cellulose nanocrystals crosslinked with sulfosuccinic acid as sustainable proton exchange membranes for electrochemical energy applications. Membranes (Basel). 2022; 12(7):658. https://doi.org/10.3390/membranes12070658 PMid:35877861 PMCid:PMC9319731.
17. Kang N-W, Yoon S-Y, Kim S, Yu N-Y, Park J-H, Lee J-Y, *et al*. Subcutaneously injectable hyaluronic acid hydrogel for sustained release of donepezil with reduced initial burst release: Effect of hybridization of microstructured lipid carriers and albumin. Pharmaceutics. 2021; 13(6):864. https://doi.org/10.3390/pharmaceutics13060864 PMid:34208289 PMCid:PMC8230846.
18. Gilchrist AM, Wang P, Carreira-Barral I, Alonso-Carrillo D, Wu X, Quesada R, *et al*. Supramolecular methods: The 8-hydroxypyrene-1,3,6-trisulfonic acid (HPTS) transport assay. Supramol Chem. 2021; 33(7):325-344. https://doi.org/10.1080/10610278.2021.1999956
19. Haggag MG, Shafaa MW, Kareem HS, El-Gamil AM, El-Hendawy HH. Screening and enhancement of the antimicrobial activity of some plant oils using liposomes as nanoscale carrier. Bull Natl Res Cent. 2021; 45(1). https://doi.org/10.1186/s42269-021-00497-y
20. Dhiman J. Novel drug delivery system: Brief review. J Drug Deliv Ther. 2023; 13(11):188-196. https://doi.org/10.22270/jddt.v13i11.6023
21. Camilo CJJ, Leite DOD, Silva ARA, Menezes IRA, Coutinho HDM, Costa JGM. Lipid vesicles: Applications, principal components and methods used in their formulations: A review. Acta Biol Colomb. 2020; 25(2):339-352. https://doi.org/10.15446/abc.v25n2.74830
22. Abdellatif AAH, El-Telbany DFA, Zayed G, Al-Sawahli MM. Hydrogel containing PEG-coated fluconazole nanoparticles with enhanced solubility and antifungal activity. J Pharm Innov. 2019; 14(2):112-122. https://doi.org/10.1007/s12247-018-9335-z
23. Huang G, Huang H. Application of hyaluronic acid as carriers in drug delivery. Drug Deliv. 2018; 25(1):766-772. https://doi.org/10.1080/10717544.2018.1450910 PMid:29536778 PMCid:PMC6058522.
24. Austin J, Minelli C, Hamilton D, Wywijas M, Jones HJ. Nanoparticle number concentration measurements by multi-angle dynamic light scattering. J Nanopart Res. 2020; 22(5). https://doi.org/10.1007/s11051-020-04840-8
25. Lucchetti D, Battaglia A, Ricciardi-Tenore C, Colella F, Perelli L, De Maria R, *et al*. Measuring extracellular vesicles by conventional flow cytometry: Dream or reality? Int J Mol Sci. 2020; 21(17):6257. https://doi.org/10.3390/ijms21176257 Mid:32872424 PMCid:PMC7503575.
26. Farkas N, Kramar JA. Dynamic light scattering distributions by any means. J Nanopart Res. 2021; 23(5). https://doi.org/10.1007/s11051-021-05220-6 PMid:39381776 PMCid:PMC11459661.
27. Jin L, Jarand CW, Brader ML, Reed WF. Angle-dependent effects in DLS measurements of polydisperse particles. Meas Sci Technol. 2022; 33(4):045202. https://doi.org/10.1088/1361-6501/ac42b2
28. Lunardi CN, Gomes AJ, Rocha FS, De Tommaso J, Patience GS. Experimental methods in chemical engineering: Zeta potential. Can J Chem Eng. 2021; 99(3):627-639. https://doi.org/10.1002/cjce.23914 PMCid:PMC12140272.
29. Serrano-Lotina A, Portela R, Baeza P, Alcolea-Rodriguez V, Villarroel M, Ávila P. Zeta potential as a tool for functional materials development. Catal Today. 2023; 423(113862):113862. https://doi.org/10.1016/j.cattod.2022.08.004
30. Ramaye Y, Dabrio M, Roebben G, Kestens V. Development and validation of optical methods for zeta potential determination of silica and polystyrene particles in aqueous suspensions. Materials (Basel). 2021; 14(2):290. https://doi.org/10.3390/ma14020290 PMid:33429974 PMCid:PMC7827561.
31. Ghomrasni NB. Identification et caractérisation métrologique des nanoparticules en matrices complexes. Hal.Science. [cited 2025 Nov 28]. Available from: https://theses.hal.science/tel-03447274
32. Probst PT, Mayer M, Gupta V, Steiner AM, Zhou Z, Auernhammer GK, *et al*. Mechano-tunable chiral metasurfaces via colloidal assembly. Nat Mater. 2021; 20(7):1024-1028. https://doi.org/10.1038/s41563-021-00991-8 PMid:33927391.
33. Gordillo-Galeano A, Mora-Huertas CE. Hydrodynamic diameter and zeta potential of nanostructured lipid carriers: Emphasizing some parameters for correct measurements. Colloids Surf A Physicochem Eng Asp. 2021; 620(126610):126610. https://doi.org/10.1016/j.colsurfa.2021.126610
34. Eladawy NO, Morsi NM, Shamma RN. Diacerein-loaded hyaluosomes as a dual-function platform for

osteoarthritis management via intra-articular injection: *In vitro* characterization and *in vivo* assessment in a rat model. Pharmaceutics. 2021; 13(6):765. https://doi.org/10.3390/pharmaceutics13060765 PMid:34063749 PMCid:PMC8223785.
35. Cadete A, Olivera A, Besev M, Dhal PK, Gonçalves L, Almeida AJ, *et al*. Self-assembled hyaluronan nanocapsules for the intracellular delivery of anticancer drugs. Sci Rep. 2019; 9(1):11565. https://doi.org/10.1038/s41598-019-47995-8 PMid:31399627 PMCid:PMC6689112.
36. Moscardini A, Di Pietro S, Signore G, Parlanti P, Santi M, Gemmi M, *et al*. Uranium-free X solution: A new generation contrast agent for the ultrastructure of biological samples. Sci Rep. 2020; 10(1). https://doi.org/10.1038/s41598-020-68405-4 PMid:32665608 PMCid:PMC7360580.
37. Sahiro K, Kawato Y, Koike K, Sano T, Nakai T, Sadakane M. Preyssler-type phosphotungstate is a new family of negative-staining reagents for the TEM observation of viruses. Sci Rep. 2022; 12(1). https://doi.org/10.1038/s41598-022-11405-3 PMid:35551198 PMCid:PMC9098496.
38. Zhang H, Liu H, Wei J, Dang Y, Wang Y, Yang Q, *et al*. Single-dose recombinant VSV-based vaccine elicits robust and durable neutralizing antibody against Hantaan virus. NPJ Vaccines. 2024; 9(1). https://doi.org/10.1038/s41541-024-00814-2 PMid:38341504 PMCid:PMC10858903.
39. Kwon Y, Park J. Methods to analyze extracellular vesicles at single particle level. Micro Nano Syst Lett. 2022; 10(1). https://doi.org/10.1186/s40486-022-00156-5
40. Harrison NA, Gardner CL, da Silva DR, Gonzalez CF, Lorca GL. Identification of biomarkers for systemic distribution of nanovesicles from *Lactobacillus johnsonii* N6.2. Front Immunol. 2021; 12(723433). https://doi.org/10.3389/fimmu.2021.723433 PMid:34531870 PMCid:PMC8438180.
41. Chiang C-Y, Chen C. Toward characterizing extracellular vesicles at a single-particle level. J Biomed Sci. 2019; 26(1). https://doi.org/10.1186/s12929-019-0502-4 PMid:30646920 PMCid:PMC6332877.
42. Weiss A, Meissner AF, Boros FA, Regensburger M, Taudte RV, Matamoros-Angles A, *et al*. Transmission electron microscopy-based characterization of extracellular vesicles from plasma and serum from parkinson's disease patients. Cell Commun Signal. 2025; 23(1). https://doi.org/10.1186/s12964-025-02383-w PMid:40968382 PMCid:PMC12445024.
43. Vadivel E, Dabholkar PP. Isolation and characterization of mucilage from cinnamon Verum. Int J Pharm Sci Drug Res. 2018; 10(4):213-216. https://doi.org/10.25004/IJPSDR.2018.100402
44. Siddiqui B, Rehman AU, Haq I-U, Ahmad NM, Ahmed N. Development, optimisation, and evaluation of nanoencapsulated diacerein emulgel for potential use in osteoarthritis. J Microencapsul. 2020; 37(8):595-608. h ttps://doi.org/10.1080/02652048.2020.1829140 PMid:32981415
45. Ostróżka-Cieślik A, Wilczyński S, Dolińska B. Hydrogel formulations for topical insulin application: Preparation, characterization and *in vitro* permeation across the Strat-M® membrane. Polymers (Basel). 2023;15(17):3639. https://doi.org/10.3390/polym15173639 PMid:37688265 PMCid:PMC10489751.
46. Asghar A, Aamir MN, Sheikh FA, Ahmad N, Alotaibi NF, Bukhari SNA. Preparation, characterization of pregabalin and *Withania coagulans* extract-loaded topical gel and their comparative effect on burn injury. Gels. 2022; 8(7):402. https://doi.org/10.3390/gels8070402 PMid:35877487 PMCid:PMC9318109.
47. Ghica MV, Hîrjău M, Lupuleasa D, Dinu-Pîrvu C-E. Flow and thixotropic parameters for rheological characterization of hydrogels. Molecules. 2016; 21(6):786. https://doi.org/10.3390/molecules21060786 PMid:27322222 PMCid:PMC6273008.
48. Abedi F, Davaran S, Hekmati M, Akbarzadeh A, Baradaran B, Moghaddam SV. An improved method in fabrication of smart dual-responsive nanogels for controlled release of doxorubicin and curcumin in HT-29 colon cancer cells. J Nanobiotechnology. 2021; 19(1). https://doi.org/10.1186/s12951-020-00764-6 PMid:33422062 PMCid:PMC7797119.
49. Hanieh PN, Forte J, Di Meo C, Ammendolia MG, Del Favero E, Cantù L, *et al*. Hyaluronic acid derivative effect on niosomal coating and interaction with cellular mimetic membranes. Molecules. 2021; 26(11):3434. https://doi.org/10.3390/molecules26113434 PMid:34198955 PMCid:PMC8201220.
50. Mansoori B, Mohammadi A, Abedi-Gaballu F, Abbaspour S, Ghasabi M, Yekta R, *et al*. Hyaluronic acid-decorated liposomal nanoparticles for targeted delivery of 5-fluorouracil into HT-29 colorectal cancer cells. J Cell Physiol. 2020; 235(10):6817-6830. https://doi.org/10.1002/jcp.29576 PMid:31989649 PMCid:PMC7384933.
51. Zariwala MG, Bendre H, Markiv A, Farnaud S, Renshaw D, Taylor KM, *et al*. Hydrophobically modified chitosan nanoliposomes for intestinal drug delivery. Int J Nanomedicine. 2018;13:5837-5848. https://doi.org/10.2147/IJN.S166901 PMid:30310283 PMCid:PMC6166747.

## Author Contribution

Conceptualisation, Akanksha Chandra; Writing-review and editing, Rishabh Malviya. Both authors have read and agreed to the published version of the manuscript.